J Sci Comput (2018) 75:687–712
https://doi.org/10.1007/s10915-017-0552-2

On the Operator Splitting and Integral Equation Preconditioned Deferred Correction Methods for the "Good" Boussinesq Equation

Cheng Zhang[1] · **Jingfang Huang**[2] · **Cheng Wang**[3] · **Xingye Yue**[1]

Received: 3 September 2016 / Revised: 17 August 2017 / Accepted: 1 September 2017 /
Published online: 11 September 2017

Abstract We study two numerical methods for the "Good" Boussinesq (GB) equation. Both methods are designed to solve the spatial-temporal pseudo-spectral collocation formulations of the GB equation using the deferred correction methods in one time marching step, where the Fourier series based pseudo-spectral formulation is applied in the spatial direction. The main idea is to iteratively apply a low order method to solve an error equation and refine the provisional solutions until they converge to the high order pseudo-spectral solutions both in space and time. In the first method, an operator splitting approach is introduced as the low order preconditioner in the deferred correction procedure for the temporal Gauss collocation formulation of the original GB equation. The method shows good numerical properties when the deferred correction procedure is convergent and the accuracy requirement is achievable. However, due to the stiffness of the linear differential operators, the Krylov deferred correction (KDC) method has to be applied in order to make the iterations converge. And also, due to the spectral differentiation operator involved, the condition number of the algorithm scales as $O(N^4)$, where N is the number of Fourier terms in the spatial direction. To improve the numerical stability and efficiency, an integral equation approach is applied to "precondition" the GB equation in the second proposed numerical method, by inverting the linear terms

✉ Jingfang Huang
huang@email.unc.edu

Cheng Zhang
zhangcheng@163.com

Cheng Wang
cwang1@umassd.edu

Xingye Yue
xyyue@suda.edu.cn

1 School of Mathematical Sciences, Soochow University, Suzhou 215006, Jiangsu, People's Republic of China

2 Department of Mathematics, University of North Carolina, Chapel Hill, NC 27599, USA

3 Department of Mathematics, University of Massachusetts Dartmouth, North Dartmouth, MA 02747, USA

of the GB equation analytically. As the nonlinear term of the GB equation is non-stiff, the simple forward Euler's method preconditioned spectral deferred correction (SDC) iterations converge more efficiently than existing Jacobian-Free Newton–Krylov (JFNK) based KDC implementations, and the condition number of the new formulation is $O(1)$, which leads to a machine precision accuracy at each discrete time step.

Keywords "Good" Boussinesq equation · Deferred correction methods · Collocation formulations · Preconditioners · Integral equation method

Mathematics Subject Classification 65B05 · 65M70 · 65M12

1 Introduction

Similar to the Korteweg–de Vries (KdV) [8,22,43], Camassa-Holm [13], and cubic Schödinger equations [39], the solitary traveling wave solutions have also been discovered for the "Good" Boussinesq (GB) equation [7]

$$u_{tt} = -u_{xxxx} + u_{xx} + (u^p)_{xx}, \quad \text{integer } p \geq 2. \tag{1}$$

Applications of the GB equation include the study of interactions between surface waves and offshore structures in coastal engineering, and the design and control of water channels in hydraulics studies; see the detailed descriptions in [28,47,50] and references therein.

There have been extensive numerical studies for the GB equation. For example, a few numerical simulation results are presented in [2,9,10], while a theoretical analysis is not available in these works. A closed form solution for the two soliton interaction was obtained by Manoranjan et al. in [49] and a few numerical experiments were performed based on the Petrov-Galerkin method with linear "hat" functions. Regarding the numerical analysis for the GB equation, the stability and convergence analysis of a finite difference method is presented in [53]. In the area of pseudo-spectral scheme with periodic boundary conditions, it is worth mentioning Frutos et al.'s work [52], in which a second order temporal discretization was proposed and analyzed, and a full order convergence was proved in a weak energy norm: an L^2 norm of u combined with an H^{-2} norm of $v = u_t$. This energy norm is much weaker than the one reported in [48], where the linear part was analyzed: an H^2 norm of u combined with an L^2 norm of $v = u_t$. An alternative second order (in time) scheme is proposed and analyzed in a more recent article [17], and the convergence in the stronger energy norm (given by [48]) is established, with the help of aliasing error control techniques in the Fourier pseudo-spectral space.

Existing analytical and numerical results reveal that there exists a highly complicated interaction mechanism for the soliton-producing GB equation. In order to capture the details of the solitary wave interactions more accurately, we introduce two numerical methods for solving the GB equation in this paper, using pseudo-spectral collocation formulations in both space and time for one time marching step. In the spatial direction, the Fourier series is applied to discretize the spatial differential operators, and the nonlinear term of the GB equation is computed using the pseudo-spectral collocation scheme; in the temporal direction, the orthogonal polynomial based collocation formulations are applied so that the interpolating polynomials satisfy the GB equation exactly at the node points. Instead of the expensive Newton's method with direct Gauss elimination, our approaches use different deferred correction techniques to efficiently solve the collocation formulations, by using a lower order

method to derive the provisional solutions, and then iteratively refine the provisional solutions by estimating the errors (defects) using (not necessarily the same) lower order method. The two methods differ in the choices of deferred correction schemes, lower order method based preconditioners, and most importantly, different error equation reformulations. In the first method, an operator splitting scheme [62] is applied as the lower order method preconditioner to solve the standard error equation for the temporal Gauss collocation formulation of the original differential GB equation. Due to the stiffness of the spatial linear differential operators, we show that the spectral deferred correction (SDC) method [24] cannot converge efficiently to the collocation formulation solutions, and the Jacobian-Free Newton–Krylov (JFNK) [41,42] based Krylov deferred correction (KDC) method [36,37] has to be used. Also, for large number N of the Fourier series expansion terms, the condition number of the first algorithm scales as $O(N^4)$, resulting in larger errors for larger N. To further improve the stability and accuracy, in the second method, we apply the integral equation method (IEM) to analytically invert the linear terms in the error equation of the GB equation. The numerical results reveal that the condition number of this IEM reformulation is $O(1)$ and a machine precision accuracy is achievable for the discretized algebraic system in one time marching step. Also, as the nonlinear term in the GB equation is non-stiff, the SDC method with the simple forward Euler's scheme for the integral form error equation converges more efficiently than existing JFNK based KDC solvers. To the authors' knowledge, these spatial-temporal pseudo-spectral formulations in our methods have not been applied to the GB equation in previous research. This is the primary contribution of this paper.

This paper is organized as follows. In Sect. 2, we present the spatial-temporal pseudo-spectral discretization of the GB equation. In Sect. 3, we show the general framework of the spectral deferred correction and Krylov deferred correction methods. In Sect. 4, we present our first method, which directly applies the lower order operator splitting technique based Krylov deferred correction method to the original GB equation. Numerical results are also presented to demonstrate the accuracy, efficiency, and stability properties of the algorithm. To improve the stability and efficiency of the numerical solutions, we introduce our second method in Sect. 5, based on an integral equation reformulation of GB's error equation. Numerical results are presented to show how the stiffness from the linear terms are removed and the convergence of the SDC method compared with KDC method. In Sect. 6, we present numerical results to compare our methods with a previously implemented temporal second order operator splitting scheme in [62]. Finally in Sect. 7, we summarize our results and discuss possible strategies to further improve the numerical algorithms for the GB equation and generalization of the algorithms to other applications.

2 Spatial-Temporal Pseudo-spectral Formulation

We discuss the spatial-temporal pseudo-spectral discretization of the GB equation in this section. We first reformulate the GB equation as a temporal first order system, by introducing a new variable $v = u_t$,

$$\begin{cases} u_t = v, & (x,t) \in [-L, L] \times [0, T], \\ v_t = -u_{xxxx} + u_{xx} + (u^p)_{xx}, & (x,t) \in [-L, L] \times [0, T], \end{cases} \tag{2}$$

with given initial values $u(x, 0) = u_0(x)$, $v(x, 0) = v_0(x)$, and periodic boundary condition in the interval $[-L, L]$.

We look at one time marching step $[0, \Delta t]$. To discretize Eq. (2), we divide the interval $[-L, L]$ uniformly into $2N$ subintervals, and the nodes x_n, $n = -N, \cdots, N-1$ are given by $x_n = nh$ where $h = L/N$ is the spatial step size. In the temporal direction, we consider K (linearly scaled) Gauss nodes $\{t_k, k = 1, \cdots, K\}$ in the interval $[0, \Delta t]$. The unknowns are $u_{n,k}$ and $v_{n,k}$, representing the values of u and v in the physical domain at node point (x_n, t_k).

In the pseudo-spectral formulation, given $u_{n,k}$ and $v_{n,k}$ at different node points, one can approximate the solutions $u(x,t)$ and $v(x,t)$ using (truncated) series expansions as

$$u(x,t) \approx \sum_{n=-N}^{N-1} a_n(t) e^{in\pi x/L}, \quad v(x,t) \approx \sum_{n=-N}^{N-1} b_n(t) e^{in\pi x/L}, \tag{3}$$

where the Fourier series coefficients are given by

$$a_n(t) = \sum_{k=0}^{K} a_{n,k} L_k(t), \quad b_n(t) = \sum_{k=0}^{K} b_{n,k} L_k(t), \tag{4}$$

and L_k is the Legendre polynomial of degree k. Note that the coefficients $a_{n,k}$ and $b_{n,k}$ can be computed by first applying the fast Fourier transform (FFT) in space to $\{u_{n,k}\}_{n=-N}^{N-1}$ and $\{v_{n,k}\}_{n=-N}^{N-1}$ to derive $a_n(t_k)$ and $b_n(t_k)$ at different temporal nodes $t_k, k = 0, \cdots, K$, and then for each n, constructing the Legendre interpolating polynomial in Eq. (4) using the values $\{a_n(t_k)\}_{k=0}^{K}$ and $\{b_n(t_k)\}_{k=0}^{K}$ where the coefficients can be evaluated stably by applying the Gaussian quadrature rule directly or by using the fast Legendre transform (FLT) algorithm [25] when K is large. The temporal *Gauss collocation formulation* at each temporal node t_k for the spatial Fourier coefficients is therefore given by

$$\begin{cases} a_n'(t_k) = b_n(t_k), \\ b_n'(t_k) = \left(-(n\pi/L)^4 - (n\pi/L)^2\right) a_n(t_k) - (n\pi/L)^2 f_n(t_k) \end{cases} \tag{5}$$

for $n = -N, \cdots, N-1$, where $f_n(t_k)$ is the n-th Fourier coefficient of the nonlinear term $u^p(x,t)$ computed by applying the FFT algorithm to the function values $\{u_{j,k}^p\}_{j=-N}^{N-1}$ directly, and $a_n'(t_k)$ and $b_n'(t_k)$ can be computed by differentiating the interpolating Legendre polynomials in Eq. (4) and then evaluating the resulting polynomials at t_k.

Assuming the solutions $u(x,t)$ and $v(x,t)$ are smooth functions and the collocation formulation in Eq. (5) is solved exactly for the truncated Fourier series expansion, it is well known that when the numbers N and K increase, the numerical errors in the time interval $[0, \Delta t]$ decay exponentially fast [14,30]. Also, for each time marching step, the orthogonal polynomial based collocation formulations for solving the ordinary differential equation (ODE) system in Eq. (5) in the time interval $[0, \Delta t]$ have been well studied. When the Gauss nodes are used in $[0, \Delta t]$, the temporal *Gauss collocation method*, also referred to as the Gauss Runge–Kutta (GRK) or Gauss differential quadrature (GDQ) method [16,34,35], has the following nice numerical properties for general ODE initial value problems:

Theorem 1 *For ODE initial value problems, the Gauss collocation formulation using K nodes is of order $2K$ (super convergence), A-stable, B-stable, symplectic (structure preserving), and symmetric (time reversible).*

We refer interested readers to [5,35] for the proof of these properties, which allow very large time step size Δt when marching in time.

We also want to mention that, instead of the differential equation form in Eq. (5) for the temporal direction, the (discretized) Picard integral equation can be used as follows:

$$\begin{cases} a_n(t_k) = a_n(0) + \int_0^{t_k} b_n(\tau) d\tau, \\ b_n(t_k) = b_n(0) + \int_0^{t_k} \left(\left(-(n\pi/L)^4 - (n\pi/L)^2 \right) a_n(\tau) - (n\pi/L)^2 f_n(\tau) \right) d\tau. \end{cases} \tag{6}$$

In this integral equation formulation, instead of the numerically unstable spectral differentiation, the backward stable spectral integration matrix can be precomputed for evaluating the Legendre polynomial expansion $\int_0^{t_k} c_k L_k(\tau) d\tau$. Properties and applications of the spectral integration based numerical schemes have been studied in [24,31].

3 Spectral and Krylov Deferred Correction Methods

Despite of the nice properties of the temporal pseudo-spectral collocation formulations for initial value problems, higher order ($K \geq 10$ node points) collocation formulations are rarely used in most of today's numerical simulations. The main reason is the algorithm efficiency. Taking the ODE system in Eq. (5) as an example, if K Gauss nodes are used in the Gauss collocation formulation, we see that the solutions at temporal node t_j depend on the solutions at all node points t_k, $k = 0, \cdots, K$ (as the spectral differentiation and integration matrices are dense). In turn, a direct calculation shows that $O((NK)^3)$ operations are required if we use the Newton's method and direct Gauss elimination for each linearized system. This number increases cubicly as K increases. On the other hand, for most backward differentiation formula (BDF) type methods [1,11,55], the number of operations is only $O(N^\alpha)$ for each time step, with $\alpha \leq 3$ ($\alpha = 3$ when Newton's method and direct Gauss elimination are applied to solve the spatial nonlinear equations, and $\alpha = 1$ when fast algorithms are applied to special systems). Another difficulty associated with the temporal pseudo-spectral formulation is that, when the time step size becomes large, the initial values may no longer serve as good initial guesses for the solutions in one time interval, resulting in bad convergence in the nonlinear solver. Instead of direct Gauss elimination, an alternative approach is to use deferred correction methods to improve the efficiency by solving the discretized collocation formulations iteratively. This idea has been extensively studied mostly for ODE initial value problems in the past [3,4,12,20,24,37,38,51,54], and numerical results show that the deferred correction approaches are very competitive, in comparison with other types of initial value problem solvers, especially when very high accuracy results are required. In this section, we present the general frameworks of the spectral deferred correction (SDC) and closely related Krylov deferred correction (KDC) methods.

3.1 Lower Order Operator Splitting Scheme for a Provisional Solution

The first step of a deferred correction method is to derive provisional solutions using a lower order time march scheme. In both our algorithms, we apply the second order Strang operator splitting scheme [59] to the first order temporal form of the GB equation presented in Eq. (2). Assuming the solutions $u_{n,k}$ and $v_{n,k}$ are available at time t_k for all nodes x_n, $n = -N, \cdots, N-1$, the Strang operator splitting derives the solutions $u_{n,k+1}$ and $v_{n,k+1}$ at time t_{k+1} by the following three steps.

Strang Splitting Step 1 March the nonlinear term from t_k to $t_{k+1/2} = t_k + \frac{1}{2}\Delta t_k (\Delta t_k = t_{k+1} - t_k)$ by solving the initial value problem for $u^{(1)}$ and $v^{(1)}$:

$$\begin{cases} \partial_t u^{(1)} = 0, \quad t \in (t_k, t_{k+1/2}), \\ \partial_t v^{(1)} = \mathscr{D}_N^2((u^{(1)})^p), \quad t \in (t_k, t_{k+1/2}), \\ u^{(1)}(:, t_k) = u_{:,k}, \quad v^{(1)}(:, t_k) = v_{:,k}, \end{cases} \tag{7}$$

where $\mathscr{D}_N$ is the discretized ∂_x operator, computed by differentiating the truncated Fourier series expansion in the frequency domain, and then evaluating the derivatives at the interpolation points using FFT. Note that as $\partial_t u^{(1)} = 0$, the term $\mathscr{D}_N^2((u^{(1)})^p)$ is a constant in time, therefore the solutions of $u^{(1)}$ and $v^{(1)}$ can be analytically expressed as

$$u^{(1)}(:, t_{k+1/2}) = u^{(1)}(:, t_k), \quad v^{(1)}(:, t_{k+1/2}) = v^{(1)}(:, t_k) + \frac{1}{2}\Delta t \mathscr{D}_N^2((u^{(1)}(:, t_k))^p). \tag{8}$$

Strang Splitting Step 2 March the linear wave type equation from t_k to t_{k+1} by solving the following initial value problem for $u^{(2)}$ and $v^{(2)}$:

$$\begin{cases} \partial_t u^{(2)} = v^{(2)}, \quad t \in (t_k, t_{k+1}), \\ \partial_t v^{(2)} = -\mathscr{D}_N^4 u^{(2)} + \mathscr{D}_N^2 u^{(2)}, \quad t \in (t_k, t_{k+1}), \\ u^{(2)}(:, t_k) = u^{(1)}(: t_{k+1/2}), \quad v^{(2)}(:, t_k) = v^{(1)}(:, t_{k+1/2}). \end{cases} \tag{9}$$

Note that this is a constant coefficient linear system. In the spectral domain, the resulting equations for the Fourier coefficients $a_n(t)$ and $b_n(t)$ are (decoupled) ODE initial value problems which can be solved analytically (and easily) in the spectral domain, and then transformed back to the physical domain using FFT to derive $u^{(2)}(:, t_{k+1})$ and $u^{(2)}(:, t_{k+1})$.

Strang Splitting Step 3 March the nonlinear term from t_k to $t_{k+1/2}$ by finding the solutions $u^{(3)}$ and $v^{(3)}$ of the following initial value problem:

$$\begin{cases} \partial_t u^{(3)} = 0, \quad t \in (t_k, t_{k+1/2}), \\ \partial_t v^{(3)} = \mathscr{D}_N^2((u^{(3)})^p), \quad t \in (t_k, t_{k+1/2}), \\ u^{(3)}(:, t_k) = u^{(2)}(:, t_{k+1}), \quad v^{(3)}(:, t_k) = v^{(2)}(:, t_{k+1}). \end{cases} \tag{10}$$

Similar to Step 1, this system can be solved analytically as shown in the following formulas:

$$u^{(3)}(:, t_{k+1/2}) = u^{(3)}(:, t_k), \quad v^{(3)}(:, t_{k+1/2}) = v^{(3)}(:, t_k) + \frac{1}{2}\Delta t \mathscr{D}_N^2((u^{(3)}(:, t_k))^p). \tag{11}$$

We define the solutions at t_{k+1} as $u_{:,k+1} = u^{(3)}(:, t_{k+1/2})$ and $v_{:,k+1} = v^{(3)}(:, t_{k+1/2})$.

We refer interested readers to [62] for further details of this second order Strang operator splitting (OS2) scheme for the GB equation, where rigorous stability and convergence analyses were performed and validated numerically.

3.2 Error Equation

For the collocation formulation of the GB equation in Eq. (5) in the time interval $[0, \Delta t]$, starting from $t_0 = 0$, one can march step by step from t_k to t_{k+1} ($k = 0, \cdots, K-1$) using the second order Strang operator splitting technique from previous section to derive the discretized solutions $\{u_{n,k}\}_{n=-N}^{N-1}$ and $\{v_{n,k}\}_{n=-N}^{N-1}$ at the Gauss nodes $\{t_k\}_{k=1}^{K}$ that are spatially pseudo-spectrally accurate but only second order in time. Using these discretized solutions, one can construct the continuous provisional solutions using the high order/degree (order N in space and degree K in time) interpolating series expansions as in

$$\tilde{u}(x, t) = \sum_{n=-N}^{N-1} \tilde{a}_n(t) e^{in\pi x/L}, \quad \tilde{v}(x, t) = \sum_{n=-N}^{N-1} \tilde{b}_n(t) e^{in\pi x/L}, \tag{12}$$

where the Fourier series coefficients are given by

$$\tilde{a}_n(t) = \sum_{k=0}^{K} \tilde{a}_{n,k} L_k(t), \quad \tilde{b}_n(t) = \sum_{k=0}^{K} \tilde{b}_{n,k} L_k(t), \tag{13}$$

and L_k is the kth degree Legendre polynomial. For these provisional solutions $\tilde{u}(x,t)$ and $\tilde{v}(x,t)$, we can define the error (or defect) functions $\varepsilon(x,t)$ and $\delta(x,t)$ as the differences between the exact and provisional solutions as

$$u(x,t) = \tilde{u}(x,t) + \varepsilon(x,t) \text{ and } v(x,t) = \tilde{v}(x,t) + \delta(x,t). \tag{14}$$

Substituting the errors into the original GB equation gives

$$\begin{cases} \frac{\partial(\tilde{u}+\varepsilon)}{\partial t} = (\tilde{v}+\delta), \\ \frac{\partial(\tilde{v}+\delta)}{\partial t} = -(\tilde{u}+\varepsilon)_{xxxx} + (\tilde{u}+\varepsilon)_{xx} + ((\tilde{u}+\varepsilon)^p)_{xx}, \end{cases}$$

and we derive the *error equation*

$$\begin{cases} \frac{\partial \varepsilon}{\partial t} = \delta + (\tilde{v} - \tilde{u}_t), \\ \frac{\partial \delta}{\partial t} = -\varepsilon_{xxxx} + \varepsilon_{xx} + ((\tilde{u}+\varepsilon)^p - \tilde{u}^p)_{xx} + (-\tilde{u}_{xxxx} + \tilde{u}_{xx} - \tilde{v}_t + (\tilde{u}^p)_{xx}). \end{cases} \tag{15}$$

Further introducing the "residue" functions $c(t)$ and $d(t)$ as

$$c(t) = (\tilde{v} - \tilde{u}_t) \text{ and } d(t) = \left(-\tilde{u}_{xxxx} + \tilde{u}_{xx} - \tilde{v}_t + (\tilde{u}^p)_{xx}\right),$$

and noticing that one can always reconstruct $\tilde{u}(x,t)$ by integrating the approximate solution $\tilde{v}(x,t)$ as $\tilde{u}(x,t) = u(x,0) + \int_0^t \tilde{v}(x,\tau)d\tau$ to guarantee that $c(t) = (\tilde{v} - \tilde{u}_t) = 0$, we observe that the error equation can be simplified as

$$\begin{cases} \frac{\partial \varepsilon}{\partial t} = \delta \\ \frac{\partial \delta}{\partial t} = -\varepsilon_{xxxx} + \varepsilon_{xx} + ((\tilde{u}+\varepsilon)^p - \tilde{u}^p)_{xx} + d(t), \end{cases} \tag{16}$$

with initial conditions $\varepsilon(x,0) = 0$, $\delta(x,0) = 0$, and periodic boundary conditions.

In our numerical implementation, $\tilde{u}(x,t)$ from the lower order solver is always replaced by the reconstructed $\tilde{u}(x,t) = u(x,0) + \int_0^t \tilde{v}(x,\tau)d\tau$ using the computed $\tilde{v}(x,t)$ and spectral integration technique. This reconstruction projects the original lower order provisional solutions to a manifold satisfying (up to spectral accuracy) $\tilde{u}_t(x,t) = \tilde{v}(x,t)$. This changes the lower order solutions, however it keeps the convergence order of the provisional solutions.

We want to mention that, when the provisional solutions $\tilde{u}$ and $\tilde{v}$ satisfy the collocation formulation in Eq. (5), the residue function will satisfy $d(t) = 0$. As both ε and δ are zero initially at $t = 0$, clearly the analytical solutions $\varepsilon(x,t)$ and $\delta(x,t)$ will always be zero. Also, when a lower order time marching scheme is applied to solve Eq. (16) in this case, the numerical solutions are also zero, the same as the analytical solutions. Therefore, solving Eq. (5) is equivalent to finding the provisional solutions $\tilde{u}$ and $\tilde{v}$ such that when a lower order method is applied to the error equation in Eq. (16), the numerical values of ε and δ are zero.

3.3 Spectral Deferred Correction and Krylov Deferred Correction Methods

In the deferred correction schemes, a lower order method (not necessarily the same one being used to derive the provisional solutions as discussed in previous section) can be applied to solve the error equation in Eq. (16). Denoting the discretized lower order solutions of the

errors $\varepsilon(x,t)$ and $\delta(x,t)$ as $\tilde{\varepsilon}$ and $\tilde{\delta}$, these solutions can be considered as the outputs of an implicit function H defined by

$$\begin{bmatrix} \tilde{\varepsilon} \\ \tilde{\delta} \end{bmatrix} = H\left(\begin{bmatrix} \tilde{u} \\ \tilde{v} \end{bmatrix} \right), \tag{17}$$

and one deferred correction iteration for the given provisional solutions $\tilde{u}$ and $\tilde{v}$ can be considered as one evaluation of the function H, where the input variables are $\tilde{u}$ and $\tilde{v}$, and the output values are the low order estimates $\tilde{\varepsilon}$ and $\tilde{\delta}$ of the errors. Both the input variables $\tilde{u}$ and $\tilde{v}$ and output variables $\tilde{\varepsilon}$ and $\tilde{\delta}$ are of size $K \times 2N$, and the evaluation of the function H consists of K marching steps to solve the error equation in (16) at each temporal node t_k, $k = 1, \cdots, K$. We want to mention that a numerically acceptable lower order method should at least have the following two features: (1) it is easy to compute, and (2) when the residue $d(t) = 0$ (i.e., the provisional solutions $\tilde{u}$ and $\tilde{v}$ are the solutions to the Gauss collocation formulation), the lower order estimates $\tilde{\varepsilon}$ and $\tilde{\delta}$ should both be zero. Most existing linear multistep or Runge–Kutta methods have these features, and a good example is the Euler's method for time marching. We leave the details of different lower order methods to Sects. 4 and 5.

The spectral deferred correction (SDC) and Krylov deferred correction (KDC) methods apply different strategies to utilize the output lower order error estimates from the function H. In SDC, the outputs $\tilde{\varepsilon}$ and $\tilde{\delta}$ are added back to current provisional solutions $\tilde{u}$ and $\tilde{v}$ to form "improved" provisional solutions, which will be the new input variables for the function H, and this procedure continues until $\tilde{\varepsilon}$ and $\tilde{\delta}$ converge to 0, or a maximum number of function evaluations (deferred corrections) is reached. In the latter case, one usually reduces the step size Δt and restarts the deferred correction method. In [36], it was shown that for linear ODE initial value problems, the SDC method is equivalent to applying the Neumann series expansion (fixed point iteration) to a low-order method preconditioned high order collocation formulation. When the low-order method preconditioner is properly selected, the SDC method can converge efficiently. However, for stiff ODE systems or differential algebraic equation (DAE) initial value problems, analytical and numerical studies reveal that due to the existence of "bad" eigenvalues in the low-order method preconditioned system, order reductions are often observed and for many settings, the SDC iterations become divergent after the first few iterations. To remedy the slow convergence and divergence of the SDC method, in [37], the least squares based Krylov subspace iterative methods are introduced to replace the Neumann series type iterations, by applying existing Jacobian-Free Newton–Krylov (JFNK) methods [41,42] directly to find the zeros of the preconditioned system

$$\begin{bmatrix} \tilde{\varepsilon} \\ \tilde{\delta} \end{bmatrix} = H\left(\begin{bmatrix} \tilde{u} \\ \tilde{v} \end{bmatrix} \right) = \mathbf{0}.$$

It is interesting to compare the SDC method with KDC method. For a linear problem, we assume the same provisional solutions are used to start the iterations and the same lower order preconditioner is applied, and the resulting preconditioned system is denoted by $(I - C)\mathbf{x} = \mathbf{b}$. The SDC method solves this system using the Neumann series

$$\mathbf{x} = \mathbf{b} + C\mathbf{b} + C^2\mathbf{b} \cdots + C^{j-1}\mathbf{b}$$

in its first j iterations. The KDC method, on the other hand, searches for the optimal least squares solution which minimizes $||A\mathbf{x} - \mathbf{b}||$ for $\mathbf{x}$ in the Krylov subspace

$$\mathbb{K}_j(C, \mathbf{b}) = span\{\mathbf{b}, C\mathbf{b}, C^2\mathbf{b}, \cdots, C^{j-1}\mathbf{b}\}.$$

If the lower order preconditioner is effective, the spectral radius of C is small, both the SDC and KDC methods should converge efficiently. However, the SDC method only requires storage of the previous iteration solutions, while the KDC method usually needs the data storage from all history deferred correction iterations when a GMRES type method is applied as C is not symmetric in general. Also, an overhead cost is required by the KDC method when searching for the optimal solutions in the Krylov subspace, although this cost is only a small portion of the total number of operations, as the most expensive computations are usually the evaluations of the function H for the given provisional solutions. When there are a few "bad" eigenvalues in C (e.g., due to the stiffness of the initial value problem), the SDC method may either converge slowly, or become divergent. The KDC method, on the other hand, always converges.

We present the following guidelines for the choice between the SDC and KDC methods: When an optimized preconditioner designed specifically for the underling problem is available and the Neumann series expansion converges efficiently, the SDC method is recommended since it requires much less storage and no overhead operation. However, for most low-order preconditioners and general problems, we recommend the KDC method due to its much improved convergence properties. These guidelines are further demonstrated in Sects. 4 and 5 next.

Remark 1 The second order Strang splitting algorithm in Eqs. (7)–(11) is a very effective preconditioner for solving the standard error equation of the temporal pseudo-spectral collocation formulation of the GB equation, where the equations at each splitting step can be solved efficiently using the analysis based formulas. Other low-order preconditioning methods have also been studied by the authors, to better understand how to choose an "optimal" low-order preconditioner for a specific problem setting. Interested readers are referred to [46] for some preliminary comparisons of several low-order preconditioners, and to [12,15,19,21,23] for different *differential* and *algebraic* operator splitting based low-order preconditioning techniques in the SDC or closely related integral deferred correction (IDC) methods [20]. In particular, in [15,19], the alternating direction implicit (ADI) splitting technique has been successfully applied to solving time-dependent differential equations in *higher spatial* dimensions. Unfortunately for most low-order preconditioning techniques, due to the extreme stiffness of the spatial linear differential operator $\mathscr{D}_N^4$, the SDC and IDC iterations cannot efficiently converge to the solutions of the collocation formulation when using the standard error equation, and the Krylov subspace based KDC approach has to be applied to overcome this difficulty. This will be addressed in the next section.

4 Operator Splitting Preconditioned KDC Algorithm

For ease of notations and discussions, we consider a first order operator splitting technique (instead of the 2nd order Strang splitting) for solving the error equation in Eq. (16), and compare the SDC and KDC methods.

4.1 First Order Operator Splitting Preconditioner

We apply a differential operator splitting technique to solve the error equation using the following two steps when marching from $t = t_k$ to $t = t_{k+1}$.

Step I Using the initial values $\varepsilon(x, t = t_k)$ and $\delta(x, t = t_k)$, march from $t = t_k$ to $t = t_{k+1} = t_k + \Delta t_k$ by solving the linear partial differential equation system

$$\begin{cases} \frac{\partial \varepsilon^{(1)}}{\partial t} = \delta^{(1)}, \\ \frac{\partial \delta^{(1)}}{\partial t} = -\varepsilon^{(1)}_{xxxx} + \varepsilon^{(1)}_{xx} + d(t), \end{cases} \tag{18}$$

with periodic boundary conditions.

Step II Using the solutions $\varepsilon^{(1)}(:, t = t_{k+1})$ and $\delta^{(1)}(:, t = t_{k+1})$ from Step I as the initial values, march from $t = t_k$ to $t = t_{k+1}$ by solving the nonlinear ordinary differential equation system

$$\begin{cases} \frac{\partial \varepsilon}{\partial t} = 0, \\ \frac{\partial \delta}{\partial t} = ((\tilde{u} + \varepsilon)^p - \tilde{u}^p)_{xx}. \end{cases} \tag{19}$$

In this operator splitting scheme, both Eqs. (18) and (19) can be solved analytically. Similar to Steps 1 and 3 in the Strang splitting scheme, the system in Eq. (19) is a simple ODE system and the analytical solutions are the simple constant function for ε, and linear function for δ. The system in Eq. (18) is a linear partial differential equation, for periodic boundary conditions, we can represent the solutions using the Fourier series as

$$\varepsilon^{(1)}(x, t) = \sum_{n=-N}^{N-1} \eta_n(t) e^{in\pi x/L},$$
$$\delta^{(1)}(x, t) = \sum_{n=-N}^{N-1} \theta_n(t) e^{in\pi x/L},$$

with $\eta_n(t_k)$ and $\theta_n(t_k)$ the given initial conditions. To find the analytical solutions of Eq. (18) at $t = t_{k+1}$, we consider the ODE system in the spectral domain for the coefficients $\eta_n(t)$ and $\theta_n(t)$ given by

$$\begin{cases} \eta_n'(t) = \theta_n(t), \quad t \in (t_k, t_{k+1}), \\ \theta_n'(t) = -((n\pi/L)^4 + (n\pi/L)^2)\eta_n(t) + d_n(t), \quad t \in (t_k, t_{k+1}), \\ \eta_n(t_k) = \varepsilon_n(t_k), \ \theta_n(t_k) = \delta_n(t_k), \end{cases} \tag{20}$$

where $d_n(t)$ is the nth Fourier coefficient of the expansion

$$d(t) = \sum_{n=-N}^{N-1} d_n(t) e^{in\pi x/L}.$$

The system in Eq. (20) can be solved analytically, and it is straightforward to verify that

$$\begin{cases} \eta_n(t) = \eta_n(t_k)\cos(M_n(t - t_k)) + \frac{\theta_n(t_k)}{M_n}\sin(M_n(t - t_k)) + \int_{t_k}^{t} \frac{\sin(M_n(t-\tau))}{M_n} d_n(\tau) d\tau, \\ \theta_n(t) = -M_n \eta_n(t_k)\sin(M_n(t - t_k)) + \theta_n(t_k)\cos(M_n(t - t_k)) \\ \qquad + \int_{t_k}^{t} \cos(M_n(t - \tau)) d_n(\tau) d\tau, \end{cases} \tag{21}$$

where $M_n = \sqrt{(n\pi/L)^4 + (n\pi/L)^2}$. For the integrals

$$\int_{t_k}^{t} \sin(M_n(t - \tau)) d_n(\tau) d\tau, \quad \int_{t_k}^{t} \cos(M_n(t - \tau)) d_n(\tau) d\tau,$$

product rules can be applied, with the function $d_n(t)$ approximated by its linear interpolating polynomial using the function values $d_n(t_k)$ and $d_n(t_{k+1})$, and the integrals are then evaluated

analytically. Note that the coefficients which map the function values to the integral values can be precomputed and stored in the memory.

Applying this first order operator splitting technique, one can derive the lower order estimates of the errors, which are the outputs of the function H for the given provisional solutions. We then apply either the KDC or SDC method to find the roots of H, which represent the solutions of the collocation formulation at the discretized spatial and temporal nodes. If the KDC or SDC iterations are convergent and the end point Δt is not one of the node points in the collocation formulation, i.e., when the Gauss collocation formulation is applied, we define the final solutions at time Δt as

$$\begin{cases} a_n(\Delta t) = a_n(0) + \int_0^{\Delta t} b_n(\tau) d\tau, \\ b_n(\Delta t) = b_n(0) + \int_0^{\Delta t} \left(\left(-(n\pi/L)^4 - (n\pi/L)^2 \right) a_n(\tau) - (n\pi/L)^2 f_n(\tau) \right) d\tau, \end{cases} \tag{22}$$

where the integrals are evaluated using the Gauss quadrature rule and the collocation formulation solutions a_n, b_n and corresponding f_n at the Gauss node points. When Δt is one of the collocation node points (i.e., Radau IIa or Lobatto nodes), the solutions at the end point are used directly as the initial value for next time marching step.

4.2 Convergence, Stability, and Numerical Results

The SDC and KDC numerical algorithms are implemented in Matlab and the source codes are available upon request. In order to test their performance, we consider the following exact soliton solution from [17] when $p = 2$,

$$u_{exact}(x,t) = -A \operatorname{sech}^2 \left(\frac{P}{2}(x - c_0 t) \right). \tag{23}$$

where $0 < P \leq 1$ is a constant, the amplitude A and wave speed c_0 are functions of P respectively, given by

$$A = \frac{3P^2}{2}, \quad c_0 = \left(1 - P^2\right)^{1/2}. \tag{24}$$

Notice that the analytical solution decays exponentially fast when $|x| \to \infty$, we can therefore choose a large enough number L, and consider the GB equation on the interval $[-L, L]$ with periodic boundary conditions. In our numerical experiments, we set $A = 0.5$ and $L = 80$. The numbers P and C_0 are determined accordingly.

We first compare the analytical solution u_{exact} and numerically computed $\tilde{u}$ to validate our KDC solver. On the left of Fig. 1, we show the analytical and numerical values of $u(x,t)$ at time $t = 4$, and on the right, we plot the error. Our KDC method utilizes the JFNK solver downloaded from the website of the author of [40,41]. For the pseudo-spectral collocation formulation for each time interval, we use $K = 5$ Gauss nodes for each time step of size $\Delta t = 4/12$ (a total of 12 steps to march from $t = 0$ to $t = 4$) and $N = 128$ in the spatial discretization. The second order Strang splitting is applied to derive the provisional solutions initially, and the first order operator splitting is applied to get the lower order estimates of the errors in the Krylov deferred correction iterations (evaluations of H).

To understand the convergence properties of the temporal Gauss collocation formulation, we test the KDC solver for different step sizes Δt for the cases $K = 3$, $K = 4$, and $K = 5$. In the experiment, we fix $N = 128$ so that the spatial direction is resolved approximately to 12 digits accuracy as show in Fig. 1. We plot the errors for different settings in Fig. 2, where the number of time steps to march from $t = 0$ to $t = 4$ is used for the x-axis instead of Δt.

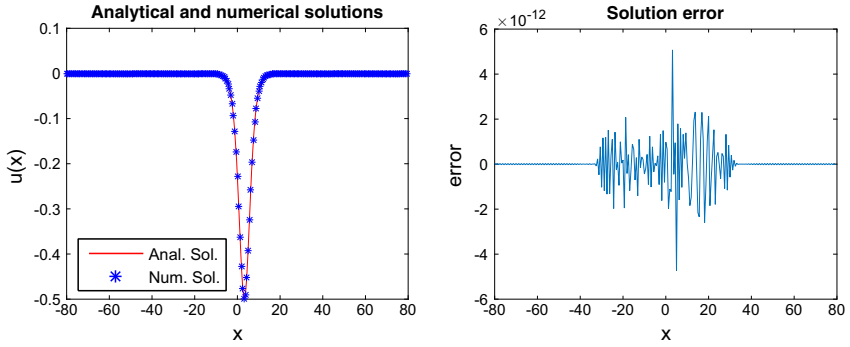

Fig. 1 Analytical and numerical solutions at $t = 4$ (left) and the numerical error (right)

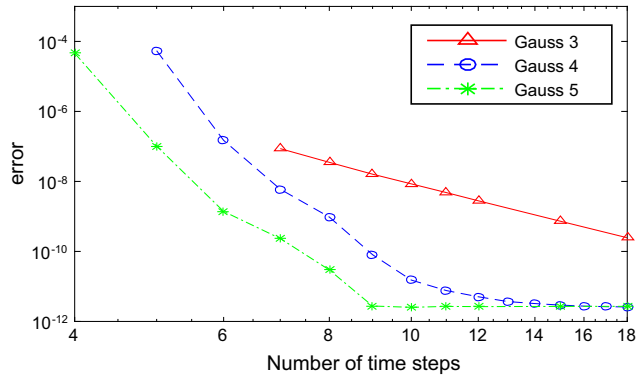

Fig. 2 Temporal convergence for different number of Gauss nodes and time step sizes

We also numerically estimate the slope of each curve corresponding to different numbers of Gauss nodes. For Gauss 3 (3 Gauss nodes), the slope is approximately 6.33, which matches the result (from traditional study of ODE initial value problems when Δt is small, see Theorem 1) that when K nodes are used, the Gauss collocation formulation should be order $2K$ in time. However, for Gauss 4 and Gauss 5, we observed much faster convergence and the slope of each curve (before reaching achievable accuracy) is approximately 15 for both cases. We believe this phenomenon is due to the pseudo-spectral nature of the Gauss collocation formulation. This issue is currently being further studied and more rigorous analysis will be provided in the future. In Table 1, we fix $N = 128$ and study how the errors decay when the number of temporal Gauss nodes increases in a single marching step from $t = 0$ to $t = 1$ ($\Delta t = 1$). From the numerical results, we see that the error decreases almost exponentially when the number of Gauss nodes increases, until it reaches the maximal achievable accuracy.

However, we also observe that when the error reaches approximately $O(10^{-12})$, no further error reduction can be achieved by adding more Gauss nodes (see $K = 12$ and $K = 13$ results in Table 1). To test if this is caused by the spatial resolution, we fix $K = 12$ and $\Delta t = 1$, and study how the errors in one time marching step decay for different numbers of spatial nodes N. The numerical results in Table 2 show that when N increases, the errors first decay, but increase rapidly after certain N ($N = 128$ in this case).

Table 1 One marching step errors for different number of Gauss nodes, KDC, $N = 128$, $\Delta t = 1$

# Gauss nodes	5	6	7	8	9
$L_\infty error$	2.86×10^{-7}	5.54×10^{-8}	4.65×10^{-9}	6.45×10^{-10}	1.14×10^{-10}
# Gauss nodes	10	11	12	13	14
$L_\infty error$	1.63×10^{-11}	4.86×10^{-12}	2.13×10^{-12}	2.04×10^{-12}	2.18×10^{-12}

Table 2 Error for different number of Fourier terms, KDC method, $K = 12$, $\Delta t = 1$

N	32	64	128	256	512	1024
L_∞ error	2.01×10^{-3}	5.90×10^{-6}	2.13×10^{-12}	3.46×10^{-10}	7.93×10^{-9}	3.57×10^{-7}

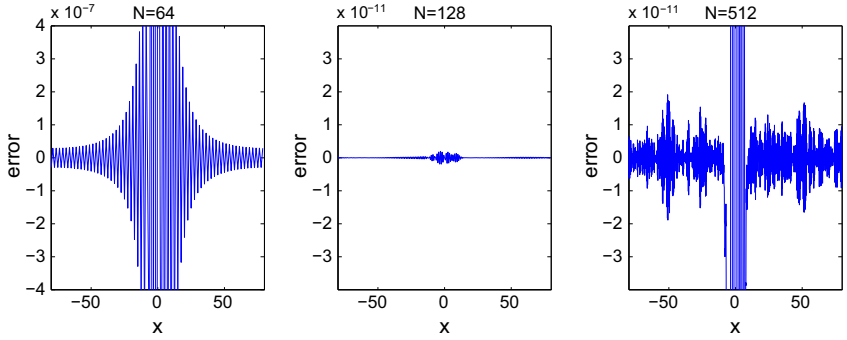

Fig. 3 N^4-instability: errors for $N = 64$ (left), $N = 128$ (middle), and $N = 512$ (right)

Our analysis shows that this error behavior is caused by the application of the differential operator on the Fourier series. Notice that both FFT and IFFT introduce machine errors ($O(10^{-15})$ relative error) in the computation. These errors will be magnified by the factor N^4 when computing $\tilde{u}_{xxxx}$ to derive $d(t) = (-\tilde{u}_{xxxx} + \tilde{u}_{xx} - \tilde{v}_t + (\tilde{u}^p)_{xx})$ in the deferred correction methods for the spatial-temporal pseudo-spectral formulation. In Fig. 3, we fix $K = 12$ and $\Delta t = 1$, and study this numerical N^4-instability in one time marching step for large N values. When $N = 64$, the solution is under-resolved and the corresponding resolution error is greater than the error from the N^4-instability (left of Fig. 3), when $N = 512$, the N^4-instability can be observed, and the best result is when $N = 128$ where the resolution errors and instability errors are balanced. The N^4-instability is not an inherent problem of the original GB equation, it is the result of the differential equation based formulation and the ill-conditioned numerical differentiation operator. In next section, we show how to avoid the N^4-instability by reformulating the GB equation into its integral form in the frequency domain.

In the previous numerical experiments, for the spatial-temporal pseudo-spectral formulation in each time step $[0, \Delta t]$, the KDC method is applied to the preconditioned system and the Newton–Krylov iterations are controlled by the black-box JFNK solver. As discussed in Sect. 3.3, in comparison with the SDC method, the KDC method usually requires more storage and some overhead operations to find the optimal solution in the Krylov subspace. In the following, we study the convergence of the KDC method and compare it with the SDC

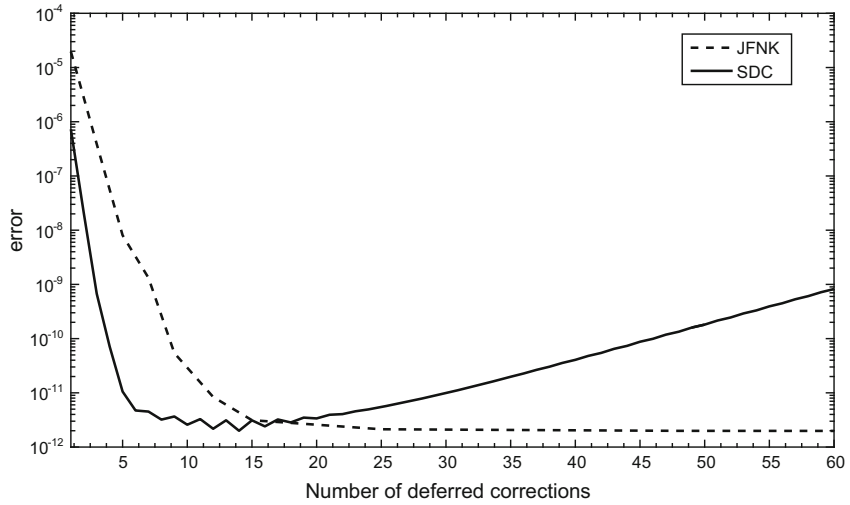

Fig. 4 Convergence of the KDC and SDC iterations, $N = 128$, $K = 12$, $\Delta t = 1$

Table 3 L_∞ error for different number of deferred corrections, SDC method, $N = 256$, $K = 12$, $\Delta t = 1$

Iteration #	1	2	3	4	5	6
$Norm([\varepsilon, \delta])$	8.44×10^{-7}	2.13×10^{-8}	7.46×10^{-10}	1.06×10^{-10}	2.25×10^{-10}	1.29×10^{-9}
Iteration #	7	8	9	10	15	20
$Norm([\varepsilon, \delta])$	9.44×10^{-9}	6.46×10^{-8}	5.85×10^{-7}	5.89×10^{-6}	2.20×10^{-1}	NaN

Table 4 L_∞ error for different number of deferred corrections, KDC method, $N = 256$, $K = 12$, $\Delta t = 1$

Iteration #	1	3	5	7	18	84
$Norm([\varepsilon, \delta])$	1.97×10^{-5}	3.88×10^{-7}	8.03×10^{-9}	1.44×10^{-9}	3.25×10^{-10}	3.47×10^{-10}

approach. In Fig. 4, we plot how the errors change as a function of the number of deferred corrections for the settings $N = 128$, $\Delta t = 1$ and $K = 12$. In Table 3, we show how the errors decay for different number of deferred correction iterations in the SDC method for the settings $N = 256$, $\Delta t = 1$, and $K = 12$. Notice that setting $N = 256$ will introduce more serious N^4-instability that propagates in the deferred correction iterations. It can be observed that the black box JFNK based KDC solver is always convergent, but due to the overhead function evaluations to search for the optimal solutions in the Newton and Krylov iterations, it requires more deferred correction iterations (H evaluations) to converge to the optimal accuracy allowed by the resolution and instability. The SDC method, on the other hand, effectively utilizes the fact that the outputs from the function evaluation H are lower order estimates of the errors and converges faster than the black box JFNK solver in the first few iterations, but becomes asymptotically divergent. When $N = 256$, our numerical results show that the solutions blow up after 20 deferred correction iterations. We refer interested readers to [56] for more detailed analysis of the divergence behaviors of the Neumann series

type SDC methods. In comparison, we show the convergence of the KDC approach in Table 4. It can be observed that the KDC method is always convergent, due to the use of the Krylov subspace to control the growth of the few bad eigenmodes. A current research topic is how to revise the black box JFNK solver, so it can have better convergence properties for finding the zeros of the "special structured" deferred correction preconditioned function H. Research along this direction will be reported in the future.

5 Integral Equation Reformulation and SDC Algorithm

For better stability, accuracy and efficiency, in this section, we introduce a reformulated GB equation using the integral equation method (IEM) and discuss its efficient solution using the SDC and KDC methods.

The IEM based numerical schemes for differential equations have been extensively studied in recent years, a small sample of existing results include the Picard integral equation based SDC, IDC, and KDC methods for ODE and DAE systems [19,24,37]; the fast algorithms accelerated integral equation formulations for the Laplace, Poisson, Yukawa, Stokes, and Helmholtz equations [18,27,45,57,61]; the fast Gauss transform and fast marching schemes for the time-dependent diffusion type equations [32,33]; and the time-domain fast multipole methods (FMMs) for the Maxwell and elastic wave equations [26,58]. Compared with traditional finite difference and finite element methods, as the Green's function is the analytical inverse of the corresponding differential operator, one immediate advantage of the IEM reformulation is its better numerical stability. The better conditioned reformulation usually allows the design of backward stable numerical schemes [60].

5.1 Integral Equation Reformulation of the GB Equation in the Fourier Domain

We present the integral equation reformulation of the GB equation in the Fourier domain, by considering the truncated Fourier series expansion of $u(x,t)$ given by $u(x,t) = \sum_{n=-N}^{N-1} a_n(t)\mathrm{e}^{\mathrm{i}n\pi x/L}$. For the nonlinear term $u^p(x,t)$, we represent its Fourier series as $u^p(x,t) = \sum_{n=-N}^{N-1} f_n(t)\mathrm{e}^{\mathrm{i}n\pi x/L}$, where $f_n(t)$ can be (backward) stably computed from $\{a_n(t)\}_{n=-N}^{N-1}$ using the FFT and IFFT transforms (the nonlinear term u^p is computed in the physical domain). Using the truncated series, the GB equation becomes a new set of equations for the coefficients $a_n(t)$ given by

$$a_n''(t) = -M_n^2 a_n(t) - f_n(t)(n\pi/L)^2 \tag{25}$$

with $M_n = \sqrt{(n\pi/L)^4 + (n\pi/L)^2}$. For the moment, assuming $f_n(t)$ is given and the initial conditions $a_n(t_k)$, $a_n'(t_k)$ are known at time $t = t_k$, then the solutions $a_n(t)$ and $a_n'(t)$ can be written as

$$\begin{cases} a_n(t) = a_n(t_k)\cos(M_n(t-t_k)) + \dfrac{a_n'(t_k)}{M_n}\sin(M_n(t-t_k)) - \displaystyle\int_{t_k}^{t} \frac{\tilde{M}_n \sin(M_n(t-\tau))}{M_n} f_n(\tau)d\tau, \\ a_n'(t) = -M_n a_n(t_k)\sin(M_n(t-t_k)) + a_n'(t_k)\cos(M_n(t-t_k)) \\ \qquad\qquad - \tilde{M}_n \displaystyle\int_{t_k}^{t} \cos(M_n(t-\tau)) f_n(\tau)d\tau, \end{cases} \tag{26}$$

with $\tilde{M}_n = (n\pi/L)^2$. To further avoid any scaling problems due to the use of M_n and $\tilde{M}_n$, we define $y_n(t) = a_n(t)$, $z_n(t) = \frac{a_n'(t)}{M_n}$, and a much better conditioned equation system can be derived as

$$\begin{cases} y_n(t) = y_n(t_k)\cos(M_n(t-t_k)) + z_n(t_k)\sin(M_n(t-t_k)) - \dfrac{\tilde{M}_n}{M_n}\displaystyle\int_{t_k}^{t} \sin(M_n(t-\tau))\, f_n(\tau)d\tau, \\ z_n(t) = -y_n(t_k)\sin(M_n(t-t_k)) + z_n(t_k)\cos(M_n(t-t_k)) \\ \qquad\quad - \dfrac{\tilde{M}_n}{M_n}\displaystyle\int_{t_k}^{t} \cos(M_n(t-\tau))\, f_n(\tau)d\tau. \end{cases} \tag{27}$$

As the density function $f_n(t)$ in the integral is also a function of the coefficients $\{a_n(t)\}_{n=-N}^{N-1}$, this equation system can be considered as a nonlinear integral equation system for the unknowns $a_n(t)$. Note that $\tilde{M}_n/M_n < 1$ and both kernels $\sin(M_n(t-\tau))$ and $\cos(M_n(t-\tau))$ are bounded functions. The machine errors from the FFT and IFFT will therefore not be magnified.

5.2 Error Equation and its Lower Order Solution

For the nonlinear integral Eq. (27), assuming the provisional solutions $\tilde{y}_n(t)$ and $\tilde{z}_n(t)$ are derived (e.g., using the Strang operator splitting), we can derive the error equation as

$$\begin{cases} \varepsilon_n(t) = -\tilde{y}_n(t) + (\tilde{y}_n(t_k)+\varepsilon_n(t_k))\cos(M_n(t-t_k)) + (\tilde{z}_n(t_k)+\delta_n(t_k))\sin(M_n(t-t_k)) \\ \qquad\quad - \dfrac{\tilde{M}_n}{M_n}\displaystyle\int_{t_k}^{t} \sin(M_n(t-\tau))((\tilde{y}+\varepsilon)^p - \tilde{y}^p)_n(\tau)d\tau \\ \qquad\quad - \dfrac{\tilde{M}_n}{M_n}\displaystyle\int_{t_k}^{t} \sin(M_n(t-\tau))(\tilde{y}^p)_n(\tau)d\tau, \\ \delta_n(t) = -\tilde{z}_n(t) - (\tilde{y}_n(t_k)+\varepsilon_n(t_k))\sin(M_n(t-t_k)) + (\tilde{z}_n(t_k)+\delta_n(t_k))\cos(M_n(t-t_k)) \\ \qquad\quad - \dfrac{\tilde{M}_n}{M_n}\displaystyle\int_{t_k}^{t} \cos(M_n(t-\tau))((\tilde{y}+\varepsilon)^p - \tilde{y}^p)_n(\tau)d\tau \\ \qquad\quad - \dfrac{\tilde{M}_n}{M_n}\displaystyle\int_{t_k}^{t} \cos(M_n(t-\tau))(\tilde{y}^p)_n(\tau)d\tau, \end{cases} \tag{28}$$

where the errors are defined as the differences between the solutions $\{y_n(t), z_n(t)\}$ and the provisional solutions $\{\tilde{y}_n(t), \tilde{z}_n(t)\}$.

To solve the unknown errors $\{\varepsilon_n(t), \delta_n(t)\}$, we apply the simple forward Euler type method (approximating the density function by a constant) to the integral terms

$$\int_{t_k}^{t} \sin(M_n(t-\tau))((\tilde{y}+\varepsilon)^p - \tilde{y}^p)_n(\tau)d\tau \text{ and } \int_{t_k}^{t} \cos(M_n(t-\tau))((\tilde{y}+\varepsilon)^p - \tilde{y}^p)_n(\tau)d\tau$$

as in

$$\begin{aligned}
&\int_{t_k}^{t} \sin(M_n(t-\tau))((\tilde{y}+\varepsilon)^p - \tilde{y}^p)_n(\tau)d\tau \\
&\quad = ((\tilde{y}(t_k)+\varepsilon(t_k))^p - (\tilde{y}(t_k))^p)_n \int_{t_k}^{t} \sin(M_n(t-\tau))d\tau \\
&\quad = \frac{1}{M_n}((\tilde{y}(t_k)+\varepsilon(t_k))^p - (\tilde{y}(t_k))^p)_n(1-\cos(M_n(t-t_k))),
\end{aligned}$$

and

$$\begin{aligned}
&\int_{t_k}^{t} \cos(M_n(t-\tau))((\tilde{y}+\varepsilon)^p - \tilde{y}^p)_n(\tau)d\tau \\
&\quad = ((\tilde{y}(t_k)+\varepsilon(t_k))^p - (\tilde{y}(t_k))^p)_n \int_{t_k}^{t} \cos(M_n(t-\tau))d\tau \\
&\quad = \frac{1}{M_n}((\tilde{y}(t_k)+\varepsilon(t_k))^p - (\tilde{y}(t_k))^p)_n \sin(M_n(t-t_k)),
\end{aligned}$$

where the function $((\tilde{y}+\varepsilon)^p - \tilde{y}^p)_n(\tau)$ is approximated by a constant function using the values at the left end point $t = t_k$, and the integrals are then evaluated analytically. The lower order estimates of the errors at t_{k+1} are then given by

$$\begin{cases}
\varepsilon_n(t_{k+1}) = -\tilde{y}_n(t_{k+1}) + (\tilde{y}_n(t_k)+\varepsilon_n(t_k))\cos(M_n\Delta t_k) + (\tilde{z}_n(t_k)+\delta_n(t_k))\sin(M_n\Delta t_k) \\
\qquad\qquad - \dfrac{\tilde{M}_n}{M_n^2}\left((\tilde{y}(t_k)+\varepsilon(t_k))^p - (\tilde{y}(t_k))^p\right)_n(1-\cos(M_n\Delta t_k)) \\
\qquad\qquad - \dfrac{\tilde{M}_n}{M_n}\displaystyle\int_{t_k}^{t_{k+1}} \sin(M_n(t_{k+1}-\tau))(\tilde{y}^p)_n(\tau)d\tau, \\
\delta_n(t_{k+1}) = -\tilde{z}_n(t_{k+1}) - (\tilde{y}_n(t_k)+\varepsilon_n(t_k))\sin(M_n\Delta t_k) + (\tilde{z}_n(t_k)+\delta_n(t_k))\cos(M_n\Delta t_k) \\
\qquad\qquad - \dfrac{\tilde{M}_n}{M_n^2}((\tilde{y}(t_k)+\varepsilon(t_k))^p - (\tilde{y}(t_k))^p)_n\sin(M_n\Delta t_k) \\
\qquad\qquad - \dfrac{\tilde{M}_n}{M_n}\displaystyle\int_{t_k}^{t_{k+1}} \cos(M_n(t_{k+1}-\tau))(\tilde{y}^p)_n(\tau)d\tau,
\end{cases} \tag{29}$$

where $\Delta t_k = t_{k+1} - t_k$. When $n = 0$, we have

$$\begin{cases}
\varepsilon_0(t_{k+1}) = -\tilde{y}_0(t_{k+1}) + \tilde{y}_0(t_k) + \varepsilon_0(t_k) + (\tilde{z}_0(t_k)+\delta_0(t_k))\Delta t_k, \\
\delta_0(t_{k+1}) = -\tilde{z}_0(t_{k+1}) + \tilde{z}_0(t_k) + \delta_0(t_k).
\end{cases} \tag{30}$$

We want to point out that higher order integration rules have to be applied to evaluate

$$\int_{t_k}^{t_{k+1}} \sin(M_n(t_{k+1}-\tau))(\tilde{y}^p)_n(\tau)d\tau.$$

In our algorithm, the interpolating Legendre polynomial of $\tilde{y}^p$ can be constructed using the Gaussian quadrature rules, and for better efficiency, a set of coefficients B_j, $j = 1, \cdots, K$, are precomputed such that

$$\int_{t_k}^{t_{k+1}} \sin(M_n(t_{k+1}-\tau))f(\tau)d\tau = \sum_{j=1}^{K} B_j f(t_j),$$

for any polynomial f with degree no more than K. The integral

$$\int_{t_k}^{t_{k+1}} \cos(M_n(t_{k+1}-\tau))(\tilde{y}^p)_n(\tau)d\tau$$

is treated similarly.

Applying the formulas in Eqs. (29) and (30), we can efficiently derive the lower order estimates of the errors, i.e., the output of the deferred correction function H, and then apply either the SDC or KDC method to find the zero of H as discussed in Sect. 3.3. Once the iterations are convergent and as the end point Δt is not one of the Gauss collocation nodes, we define the final solutions at time Δt as

$$\begin{cases} y_n(\Delta t) = y_n(0)\cos(M_n\Delta t) + z_n(0)\sin(M_n\Delta t) - \dfrac{\tilde{M}_n}{M_n}\displaystyle\int_0^{\Delta t} \sin(M_n(\Delta t-\tau))f_n(\tau)d\tau, \\ z_n(\Delta t) = -y_n(0)\sin(M_n\Delta t) + z_n(0)\cos(M_n\Delta t) - \dfrac{\tilde{M}_n}{M_n}\displaystyle\int_0^{\Delta t} \cos(M_n(\Delta t-\tau))f_n(\tau)d\tau, \end{cases} \tag{31}$$

where $\int_0^{\Delta t} \sin(M_n(\Delta t-\tau))f_n(\tau)d\tau$ is evaluated by a precomputed mapping matrix which analytically integrates the product of the kernel function $\sin(M_n(\Delta t-\tau))$ and the interpolating polynomial of the density function f_n. The integral $\int_0^{\Delta t} \cos(M_n(\Delta t-\tau))f_n(\tau)d\tau$ is treated similarly. We want to mention that, similar to the original Gauss collocation formulation, super-convergence (order $2K$) can be obtained when defining the solution at $t = \Delta t$ using Eq. (31), and this integral equation reformulation can also be considered as a "change of variable" version of a particular symplectic method.

5.3 Convergence, Stability, and Numerical Results

We first apply the SDC method to the integral equation reformulation, where the SDC iterations are terminated whenever the output of H is smaller than a prescribed accuracy requirement. We find that the SDC method converges efficiently, and it is no longer necessary to use the JFNK based KDC method for a guaranteed convergence. Similar to the previous section, we first fix $N = 256$ and test the SDC solver for different step sizes Δt for the cases $K = 3$, $K = 4$, and $K = 5$. We plot the errors for different settings in Fig. 5, where the number of time steps to march from $t = 0$ to $t = 4$ is used for the x-axis. We also numerically estimate the slope of each curve corresponding to different number of Gauss nodes. For Gauss 3 (3 Gauss nodes), Gauss 4, and Gauss 5, the slopes are respectively 7.01, 8.49, and 10.82.

To compare the error dependency on the number of temporal Gauss nodes, in Table 5, we fix $N = 256$ and study how the errors decay in a single marching step from $t = 0$ to $t = 1$ ($\Delta t = 1$) for different number of nodes. From the numerical results, we see that the error decreases to machine precision when the number of Gauss nodes increases.

Next, we fix $K = 12$ and $\Delta t = 1$, and study how the errors in one time marching step decay for different number N of spatial nodes. The numerical results in Table 6 show that when N increases, the errors decay to machine precision. Unlike the differential equation based formulation in Sect. 4, no N^4-instability is observed (compare with Table 2). In Fig. 6, we fix $K = 12$ and $\Delta t = 1$, and study the error behaviors in one time marching step for different N values. When $N = 64$, due to insufficient resolution, a numerical error of $O(10^{-7})$ is observed. When N increases, the error decays rapidly. Unlike the differential equation case, no N^4-instability is observed when $N = 512$. Notice that when enough spatial and temporal

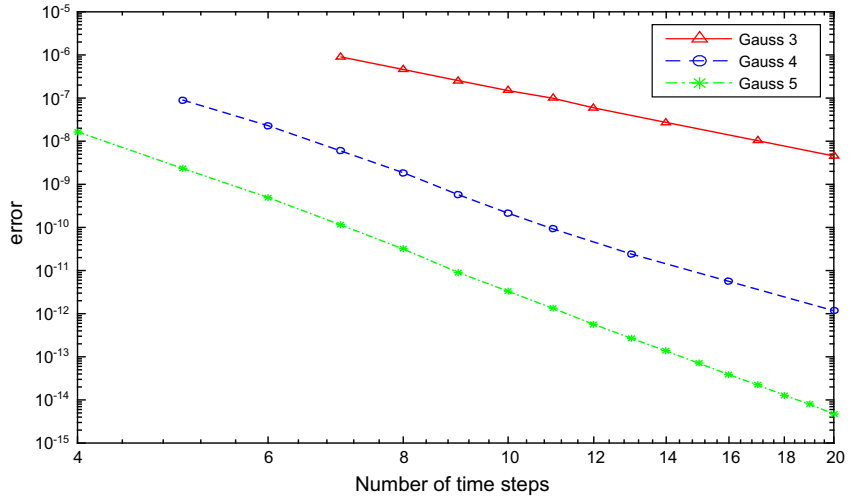

Fig. 5 Temporal convergence for different number of Gauss nodes and time step sizes, IEM-SDC

Table 5 One marching step errors for different number of Gauss nodes, IEM-SDC, $N = 256$, $\Delta t = 1$

# Gauss nodes	5	6	7	8
$L_\infty error$	5.23×10^{-9}	2.15×10^{-10}	9.20×10^{-12}	4.07×10^{-13}
# Gauss nodes	9	10	11	12
$L_\infty error$	1.80×10^{-14}	8.74×10^{-16}	1.67×10^{-16}	1.67×10^{-16}

Table 6 Error for different number of Fourier terms, IEM-SDC method, $K = 12$, $\Delta t = 1$

N	64	128	256	512
L_∞ error	5.90×10^{-6}	2.27×10^{-12}	1.67×10^{-16}	1.67×10^{-16}

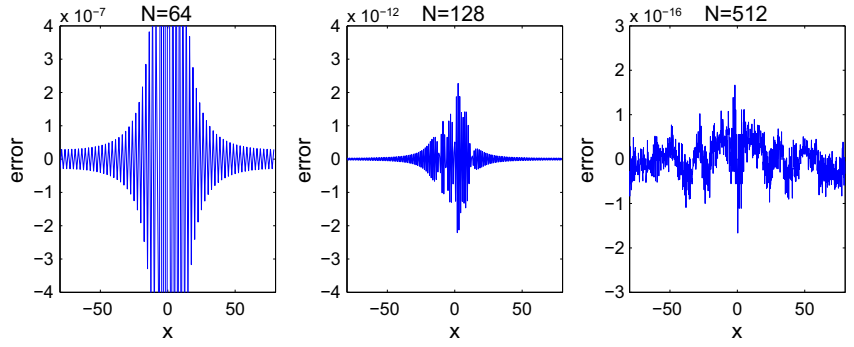

Fig. 6 Stability of SDC for the IEM reformulated GB equation: errors for $N = 64$ (left), $N = 128$ (middle), and $N = 512$ (right)

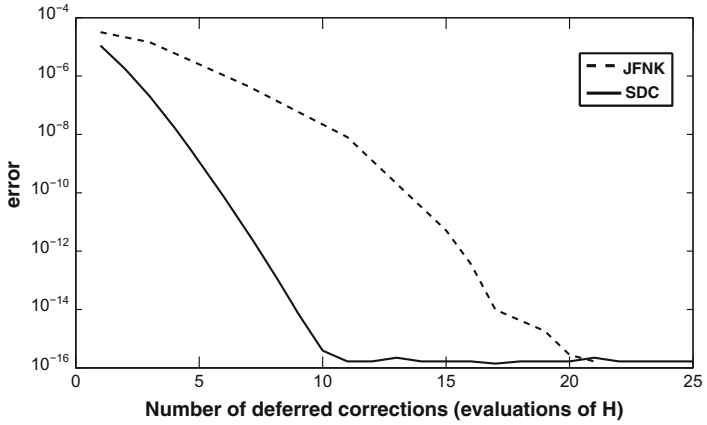

Fig. 7 Convergence of the KDC and SDC iterations, $N = 256$, $K = 12$, $\Delta t = 1$

nodes are used, we achieve machine precision accuracy. These numerical results strongly suggest that the SDC solver for the IEM reformulation of the GB equation is backward stable.

Finally, we compare the convergence of the SDC method with the black box JFNK solver based KDC approach. In Fig. 7, we plot how the errors change as a function of the number of deferred corrections for the settings $N = 256$, $\Delta t = 1$ and $K = 12$. It can be observed that, due to the overhead function evaluations to search for the optimal solution in the Newton and Krylov iterations, the black box JFNK solver requires more deferred correction iterations (H evaluations) to converge to the optimal accuracy allowed by the resolution. The SDC method, on the other hand, converges faster than the black box JFNK based KDC approach. And also, because of the better conditioned integral equation reformulation and the non-stiff nonlinear term, the SDC method is always convergent.

6 Preliminary Comparison of Different Methods

In this section, we present some preliminary results to compare the accuracy and efficiency performance of three different methods: the second order Strang operator splitting method (OS2) as discussed in [62]; the high order KDC and operator splitting collocation method (H1-KDC) for the original GB equation discussed in Sect. 4; and the high order SDC collocation method (H2-SDC) for the IEM reformulated GB equation in Sect. 5.

By combining Figs. 2 and 5, we first compare the accuracy of the solutions from two different collocation formulations in Eqs. (22) and (31). The results are shown in Fig. 8. We see that both formulations have nice accuracy properties. However, due to the N^4-instability, the original formulation can only achieve 12 digits accuracy for the specified settings, while the IEM reformulation is more stable numerically and allows machine precision accuracy when the resolution is sufficient.

Next, we compare the efficiency of the three algorithms. In Fig. 9, we consider the GB equation with analytical solution given in Eq. (23) from $t = 0$ to $t = 4$, and show the achieved accuracy as a function of the number of times the lower order time marching scheme is applied

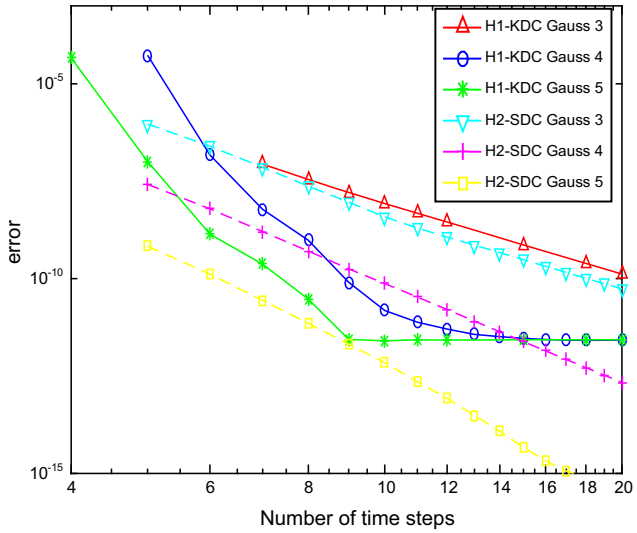

Fig. 8 A comparison between the original and IEM reformulated collocation formulations for different number of Gauss nodes and time step sizes

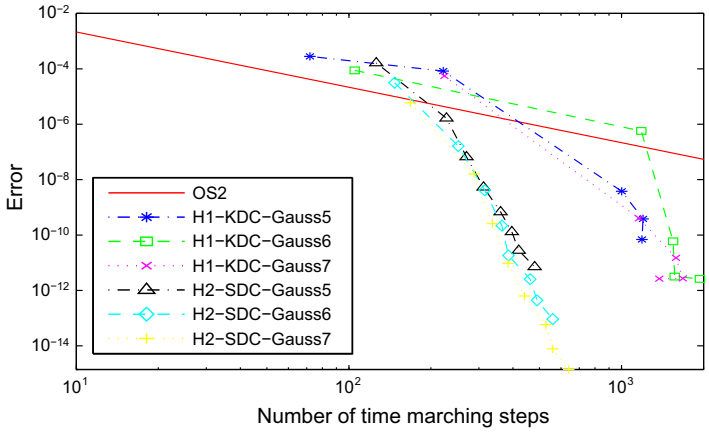

Fig. 9 Comparing the efficiency of three different algorithms

in different algorithms. Each curve represents the results using different time step sizes, and different numbers of Gauss nodes (Gauss 5, 6 and 7) are used for the original GB based KDC method (H1-KDC) and IEM-SDC formulation (H2-SDC). For H1-KDC, we set $N = 128$ to achieve the best spatial accuracy allowed by the N^4-instability as shown in Table 2. For H2-SDC, $N = 256$ is also used to fully resolve the solution to machine precision in the spatial direction. We see that for lower accuracy requirements, the second order in time operator splitting method performs well. However for higher accuracy requirements (6 or more correct digits), H2-SDC becomes the method of choice due to its efficiency and stability properties.

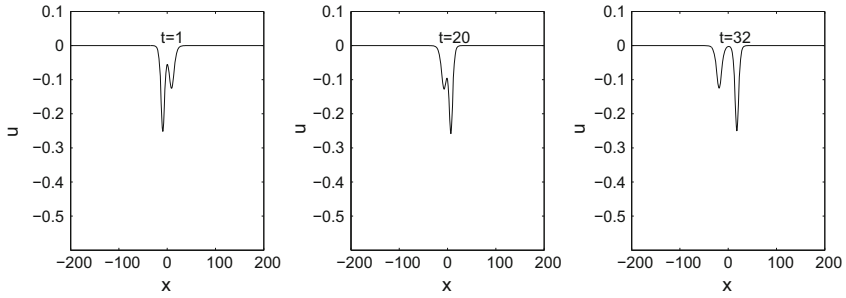

Fig. 10 Two solitons interact with each other

For H1-KDC, we observe that it is in general less efficient and less accurate, compared with H2-SDC scheme. There are several reasons for the poor performance, including (1) the N^4-instability due to spectral differentiation, (2) its relatively poor convergence properties due to the stiffness from the differential operators, and (3) the use of general purpose Jacobian-Free Newton–Krylov solver which may require some overhead function evaluations. One of our current research topics is to fine-tune the JFNK solver to take advantage of the special structures in the deferred correction formulations; results along this direction will be reported in the future.

Finally in this section, we apply these three different methods to a case where two solitons interact with each other. Utilizing the function

$$u_{two}(x,t) = -A_1 \operatorname{sech}^2\left(\frac{P_1}{2}((x-x_0)-c_1 t)\right) - A_2 \operatorname{sech}^2\left(\frac{P_2}{2}((x+x_0)+c_2 t)\right), \quad (32)$$

where

$$A_i = \frac{3P_i^2}{2}, \quad c_i = \left(1-P_i^2\right)^{1/2}, \ i = 1, 2, \quad (33)$$

with parameters $A_1 = 0.125$, $A_2 = 0.25$, $x_0 = 10$, we set the initial values of the GB equation as

$$u_0 = u_{two}(x, 0), \text{ and } v_0 = \partial_t u_{two}(x, 0).$$

In our simulation, we set $L = 200$ so that the solution is close to zero at the boundary during the simulation and the error from using the periodic boundary condition is within machine precision. In Fig. 10, we show the reference solution computed using the stable IEM-SDC (H2-SDC) method with $N = 256$ Fourier expansion terms and $K = 12$ Gauss nodes. In Fig. 11, we show how the errors grow for the collocation methods using different number of Gauss nodes ($K = 5$ and $K = 9$) with time step size $\Delta t = 1$ and $N = 256$ Fourier terms. As a comparison, we also show the results from the OS2 method with sufficient small time step size $\Delta t = 2 \times 10^{-3}$. It can be observed that, in comparison with the reference solution, the accuracy of H1-KDC with 5 Gauss nodes is similar to that of H2-SDC with the same number of Gauss nodes. With 9 Gauss nodes, H2-SDC outperforms H1-KDC in accuracy. Our numerical experiments also show that $N = 256$ is the optimal choice for H1-KDC. For larger N settings (e.g., $N = 1024$), the numerical solution blows up due to N^4-instability for H1-KDC. The H2-SDC algorithm, on the other hand, provides stable solutions for all tested N values, and it also outperforms the OS2 algorithm in efficiency in the tested accuracy regime.

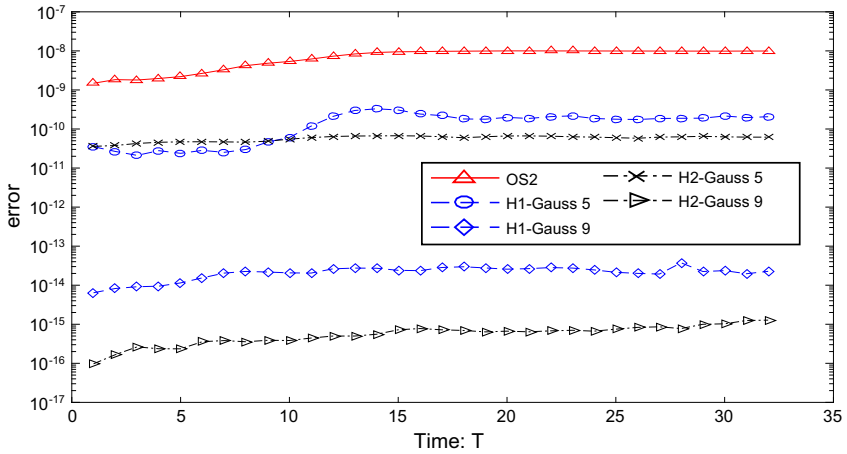

Fig. 11 How the errors grow for different methods for two solitons case

7 Conclusions and Future Work

In this paper, we present two numerical methods for the GB equation. The first method applies the Krylov deferred correction method to solve the spatial-temporal pseudo-spectral formulation of the original GB equation; and the second method reformulates the GB equation into a better conditioned integral equation system, which allows the Neumann series expansion based SDC to be applied, and leads to much better stability and efficiency for certain settings. Currently, the IEM reformulation is performed in the frequency domain. For non-periodic boundary conditions, it is possible to generalize the IEM approach to physical domain by using the physical spatial-temporal domain Green's function for the linear terms of the GB equation. Note that the nonlinear term is non-stiff, simple explicit lower order marching scheme (e.g., the forward Euler's method) can be applied in the correction procedure to derive lower order estimates of the errors, and the Neumann series expansion based SDC method converges satisfactorily.

This paper addresses the numerical solution of the *one dimensional* GB equation, however many of the numerical ideas can be generalized to higher dimensions, including the operator splitting techniques, SDC and KDC approaches, and integral equation reformulations. Of particular interest is the algebraic alternating direction implicit (ADI) splitting technique (see [15,19]), which can be considered as a special preconditioning technique so that higher dimension solutions can be derived by iteratively solving one dimensional problems. Also, for multi-dimensional problems, a better conditioned integral equation reformulation becomes even more important to reduce the storage and operations in the computer system.

The KDC, SDC, and IEM reformulation ideas can be generalized to other types of time dependent partial differential equations. Currently, these techniques are being applied to the nonlinear Schrödinger equation and time-dependent density function theory (TD-DFT). The IEM method can be applied to the linear constant coefficient terms of these equations, and if the remaining variable coefficients and nonlinear terms are non-stiff, the explicit low-order method based SDC approach can be applied to the integral equation reformulation and will yield good convergence properties. The integral equation reformulation can be considered as

an analytical preconditioner to the original PDE, which may effectively remove any numerical stiffness coming from the linear constant coefficient terms of the original equation. However, for general time dependent partial differential equations with variable coefficients or stiff nonlinear terms, the IEM preconditioner may be hard to find or inefficient to evaluate. In these cases, the KDC based approaches have to be applied in order to get better deferred correction convergence. We want to mention that there are increasing interests in fast algorithms for time-domain integral equations and integral equation based spatial variable coefficient elliptic PDE solvers, results along these directions may be adapted to further improved the accuracy and efficiency of both the SDC and KDC algorithms for more general problems.

Finally, we want to mention that other types of collocation formulations are also possible, e.g., the uniform nodes based formulation in the integral deferred correction methods [20], the exponential sums and skeletonization based collocation formulations [29,44], and those using the "prolate spheroidal wave functions" designed for "band-limited" functions in [6]. Preliminary numerical studies reveal that different formulations demonstrate different numerical behaviors, e.g., some formulations may show better accuracy properties but the convergence may be slower. It is also possible to use one particular collocation formulation for the final convergent solutions but apply several different error equation formulations in the convergence procedure. We are currently studying the mathematical and numerical properties of these formulations and their efficient combinations for optimal performance. Results along these directions will be reported in the future.

Acknowledgements C. Zhang and X. Yue were supported by NSFC-11271281, J. Huang was supported by NSF DMS-1217080, and C. Wang was supported by NSF DMS-1418689. Their supports are thankfully acknowledged.

References

1. Ascher, U.M., Petzold, L.R.: Computer Methods for Ordinary Differential Equations and Differential-Algebraic Equations. SIAM, Philadelphia (1998)
2. Attili, B.S.: The adomian decomposition method for solving the Boussinesq equation arising in water wave propagation. Numer. Methods Partial Differ. Equ. **22**(6), 1337–1347 (2006)
3. Auzinger, W., Hofstätter, H., Kreuzer, W., Weinmuller, E.: Modified defect correction algorithms for ODEs. Part I. General Theory Numer. Algorithms **36**, 135–156 (2004)
4. Auzinger, W., Hofstätter, H., Kreuzer, W., Weinmüller, E.: Modified defect correction algorithms for ODEs. Part II: stiff initial value problems. Numer. Algorithms **40**(3), 285–303 (2005)
5. Barrio, R.: On the A-stability of Runge–Kutta collocation methods based on orthogonal polynomials. SIAM J. Numer. Anal. **36**(4), 1291–1303 (1999)
6. Beylkin, G., Sandberg, K.: ODE solvers using band-limited approximations. J. Comput. Phys. **265**, 156–171 (2014)
7. Boussinesq, J.: Theorie des ondes et des remous qui se propagent le long d'un canal rectangulaire horizontal, en communiquant an liquide contenu dans ce canal de vitesses sensiblement pareilles de la surface anfond, liouvilles. J. Math. **17**, 55–108 (1872)
8. Boussinesq, J: Essai sur la théorie des eaux courantes. Imprimerie nationale (1877)
9. Bratsos, A.G.: A second order numerical scheme for the improved Boussinesq equation. Phys. Lett. A **370**(2), 145–147 (2007)
10. Bratsos, A.G.: A predictor-corrector scheme for the improved Boussinesq equation. Chaos Solitons Fractals **40**(5), 2083–2094 (2009)
11. Brenan, K.E., Campbell, S.L., Petzold, L.R.: Numerical Solution of Initial-Value Problems in Differential-Algebraic Equations. SIAM, Philadelphia (1987)
12. Bu, S., Huang, J., Minion, M.: Semi-implicit Krylov deferred correction methods for differential algebraic equations. Math. Comput. **81**(280), 2127–2157 (2012)
13. Camassa, R., Holm, D.: An integrable shallow water equation with peaked solitons. Phys. Rev. Lett. **71**(11), 1661 (1993)

14. Canuto, C., Hussaini, M.Y., Quarteroni, A., Zang, T.A.: Spectral Methods in Fluid Dynamics. Springer, New York (1988)
15. Causley, M., Christlieb, A., Wolf, E.: Method of lines transpose: an efficient unconditionally stable solver for wave propagation. J. Sci. Comput. **70**(2), 896–921 (2017)
16. Chen, W., Wang, X., Yu, Y.: Reducing the computational requirements of the differential quadrature method. Numer. Methods Partial Differ. Equ. **12**, 565–577 (1996)
17. Cheng, K., Feng, W., Gottlieb, S., Wang, C.: A fourier pseudospectral method for the good Boussinesq equation with second-order temporal accuracy. Numer. Methods Partial Differ. Equ. **31**(1), 202–224 (2015)
18. Chew, W.C.: Waves and Fields in Inhomogeneous Media, vol. 522. IEEE Press, New York (1995)
19. Christlieb, A., Liu, Y., Xu, Z.: High order operator splitting methods based on an integral deferred correction framework. J. Comput. Phys. **294**, 224–242 (2015)
20. Christlieb, A., Ong, B., Qiu, J.: Integral deferred correction methods constructed with high order Runge–Kutta integrators. Math. Comput. **79**(270), 761–783 (2010)
21. Crockatt, M., Christlieb, A., Garrett, C.K., Hauck, C.: An arbitrary-order, fully implicit, hybrid kinetic solver for linear radiative transport using integral deferred correction. J. Comput. Phys. **346**, 212–241 (2017)
22. De Jager, E.M.: On the origin of the Korteweg–de Vries equation. arXiv:math/0602661 (2006)
23. Duarte, M., Emmett, M.: High order schemes based on operator splitting and deferred corrections for stiff time dependent PDEs. arXiv:1407.0195v2 (2016)
24. Dutt, A., Greengard, L., Rokhlin, V.: Spectral deferred correction methods for ordinary differential equations. BIT Numer. Math. **40**(2), 241–266 (2000)
25. Dutt, A., Gu, M., Rokhlin, V.: Fast algorithms for polynomial interpolation, integration, and differentiation. SIAM J. Numer. Anal. **33**(5), 1689–1711 (1996)
26. Ergin, A., Shanker, B., Michielssen, E.: Time domain fast multipole methods: a pedestrian approach. IEEE Antennas Propag. Mag. **41**(4), 39–53 (1999)
27. Ethridge, F., Greengard, L.: A new fast-multipole accelerated poisson solver in two dimensions. SIAM J. Sci. Comput. **23**(3), 741–760 (2001)
28. Farah, L., Scialom, M.: On the periodic "good" Boussinesq equation. Proc. Am. Math. Soc. **138**(3), 953–964 (2010)
29. Glaser, A., Rokhlin, V.: A new class of highly accurate solvers for ordinary differential equations. J. Sci. Comput. **38**(3), 368–399 (2009)
30. Gottlieb, D., Orszag, S.S.: Numerical Analysis of Spectral Methods. SIAM, Philadelphia (1977)
31. Greengard, L.: Spectral integration and two-point boundary value problems. SIAM J. Numer. Anal. **28**, 1071–1080 (1991)
32. Greengard, L., Strain, J.: A fast algorithm for the evaluation of heat potentials. Commun. Pure Appl. Math. **43**(8), 949–963 (1990)
33. Greengard, L., Strain, J.: The fast gauss transform. SIAM J. Sci. Stat. Comput. **12**(1), 79–94 (1991)
34. Hairer, E., Hairer, M.: Gnicodes—matlab programs for geometric numerical integration. In: Frontiers in Numerical Analysis, pp. 199–240. Springer, Berlin (2003)
35. Hairer, E., Lubich, C., Wanner, G.: Geometric Numerical Integration: Structure-Preserving Algorithms for Ordinary Differential Equations, vol. 31. Springer, Berlin (2006)
36. Huang, J., Jia, J., Minion, M.: Accelerating the convergence of spectral deferred correction methods. J. Comput. Phys. **214**, 633–656 (2006)
37. Huang, J., Jia, J., Minion, M.: Arbitrary order Krylov deferred correction methods for differential algebraic equations. J. Comput. Phys. **221**(2), 739–760 (2007)
38. Jia, J., Huang, J.: Krylov deferred correction accelerated method of lines transpose for parabolic problems. J. Comput. Phys. **227**(3), 1739–1753 (2008)
39. Kato, T.: Nonlinear schrödinger equations. In: Schrödinger operators, pp. 218–263. Springer, 1989
40. Kelly, C.T.: Iterative Methods for Linear and Nonlinear Equations. SIAM, Philadelphia (1995)
41. Kelly, C.T.: Solving Nonlinear Equations with Newton's Method. SIAM, Philadelphia (2003)
42. Knoll, D.A., Keyes, D.E.: Jacobian-free Newton-Krylov methods: a survey of approaches and applications. J. Comput. Phys. **193**(2), 357–397 (2004)
43. Korteweg, D.J., De Vries, G.: Xli. On the change of form of long waves advancing in a rectangular canal, and on a new type of long stationary waves. Lond. Edinburgh Dublin Philos. Mag. J. Sci. **39**(240), 422–443 (1895)
44. Kushnir, D., Rokhlin, V.: A highly accurate solver for stiff ordinary differential equations. SIAM J. Sci. Comput. **34**(3), A1296–A1315 (2012)
45. Lai, J., Greengard, L., O'Neil, M.: Robust integral formulations for electromagnetic scattering from three-dimensional cavities. J. Comput. Phys. **345**, 1–16 (2017)

46. Layton, A., Minion, M.: Implications of the choice of predictors for semi-implicit picard integral deferred correction methods. Commun. Appl. Math. Comput. Sci. **2**(1), 1–34 (2007)
47. Linares, F., Scialom, M.: Asymptotic behavior of solutions of a generalized Boussinesq type equation. Nonlinear Anal. Theory Methods Appl. **25**(11), 1147–1158 (1995)
48. López-Marcos, J.C., Sanz-Serna, J.M.: Stability and convergence in numerical analysis. III. Linear investigation of nonlinear stability. IMA J. Numer. Anal. **7**, 71–84 (1988)
49. Manoranjan, V.S., Mitchell, A.R., Morris, J.L.: Numerical solutions of the good Boussinesq equation. SIAM J. Sci. Stat. Comput. **5**(4), 946–957 (1984)
50. Oh, S., Stefanov, A.: Improved local well-posedness for the periodic good Boussinesq equation. J. Differ. Equ. **254**(10), 4047–4065 (2013)
51. Ohmer, K.B., Stetter, H.J. (eds.): Defect Correction Methods. Theory and Applications. Springer, New York (1984)
52. Ortega, T., De Frutos, J., Sanz-Serna, J.M.: Pseudospectral method for the "good" Boussinesq equation. Math. Comput. **57**, 109–122 (1991)
53. Ortega, T., Sanz-Serna, J.M.: Nonlinear stability and convergence of finite-difference methods for the "good" Boussinesq equation. Numer. Math. **58**(1), 215–229 (1990)
54. Pereyra, V.: Iterated deferred corrections for nonlinear operator equations. Numer. Math. **10**(4), 316–323 (1967)
55. Petzold, L.R.: A description of DASSL: a differential-algebraic system solver. SAND82-8637, Sandia National Lab (1982)
56. Qu, W., Brandon, N., Chen, D., Huang, J., Kress, T.: A numerical framework for integrating deferred correction methods to solve high order collocation formulations of ODEs. J. Sci. Comput. **68**, 484–520 (2016)
57. Rokhlin, V.: Rapid solution of integral equations of classical potential theory. J. Comput. Phys. **60**(2), 187–207 (1985)
58. Shidooka, H., Otani, Y., Nishimura, N.: A time domain fast multipole boundary integral equation method for anisotropic elastodynamics in 3d. J. Appl. Mech. **11**, 109–116 (2008)
59. Strang, G.: On the construction and comparison of difference schemes. SIAM J. Numer. Anal. **5**(3), 506–517 (1968)
60. Trefethen, L.N., Bau III, D.: Numerical Linear Algebra, vol. 50. Siam, Philadelphia (1997)
61. Wang, H., Lei, T., Li, J., Huang, J., Yao, Z.: A parallel fast multipole accelerated integral equation scheme for 3d stokes equations. Int. J. Numer. Methods Eng. **70**(7), 812–839 (2007)
62. Zhang, C., Wang, H., Huang, J., Wang, C., Yue, X.: A second order operator splitting numerical scheme for the "Good" Boussinesq equation. Appl. Numer. Math. **119**, 179–193 (2017)